



# Forecasting peak smooth sunspot number of solar cycle 25: A method based on even-odd pair of solar cycle

Bharati Kakad<sup>\*</sup>, Amar Kakad

Indian Institute of Geomagnetism, New Panvel, 410218, India

## ARTICLE INFO

### Keywords:

Solar activity  
Solar cycle  
Solar cycle prediction  
Version 2.0 sunspots numbers

## ABSTRACT

The knowledge about future solar activity is necessary to plan our space-based missions. As yet, several prediction models (statistics- or dynamo-based) have been developed to forecast the peak smoothed sunspot number (SSN) of the upcoming solar cycle. Many of these data-based prediction models require sunspot number until the end of  $n$ th solar cycle to predict the peak of the solar cycle  $n + 1$ . However, one prefers to have the predictions well in advance. We propose a new data-based model that can provide information about the peak SSN (or amplitude) of solar cycle  $n + 1$ , and sum of peak SSN of solar cycle  $n + 2$  and  $n + 3$  at the end of each  $n$ th solar cycle. The solar cycles are paired using even-odd cycles, therefore in this model  $n$  is allowed to take even number. We used recently updated, Version-2, daily and monthly sunspot-number data. The area under the curve of each  $n$ th solar cycle  $[A^n]$  is estimated and used in the model together with its length and peak SSN  $[S_{\max}^n]$ . We noticed that difference in the area under the curve of solar cycles  $n$  and  $n + 1$  can be used to predict the summation of peak SSN of  $n + 2$  and  $n + 3$  solar cycles (i.e.,  $S_{\max}^{n+2} + S_{\max}^{n+3}$ ). We have tested this prediction model with both daily and monthly sunspot numbers. Our model predicts;  $S_{\max}^{24} + S_{\max}^{25} = 219.7 \pm 31$  and  $S_{\max}^{26} + S_{\max}^{27} = 229.4 \pm 31$ . As the peak SSN of solar cycle 24 is known, we get  $S_{\max}^{25} = 103.3 \pm 15$ . Further, model suggest that the solar cycle 26 and 27 would be similar or slightly stronger than solar cycle 24 and 25.

## 1. Introduction

The Sun follows a cyclic behaviour in its activity, which is clearly evident in various solar proxies like sunspot number, 10.7 cm solar flux, solar magnetic field, etc. The periodicity of approximately 11 years in sunspot number, termed as a solar cycle (SC), and 22 years in the magnetic field are widely known (Hathaway, 2015). We know that the Sun constantly emits electromagnetic radiations and energetic charged particles in the form of solar wind. Our near-Earth space is filled with these energetic particles and their interaction with the Earth's magnetic field drives different currents in the Earth's magnetosphere and ionosphere (Acero et al., 2018; Kakad et al., 2019; Ingale et al., 2019). These energetic charged particles are harmful to our space-based technology. Depending on the solar activity, we may encounter extreme space weather conditions like the Carrington event (Tsurutani et al., 2003; Lakhina and Tsurutani, 2018). As per the records, the Carrington event is the most powerful, historic geomagnetic storm recorded on the Earth, which occurred in the solar cycle 10. Such extreme space weather events have a hazardous impact on our technologically-dependent society (Riley

et al., 2018). The response of our geospace is highly controlled by the solar activity (Alves et al., 2006; Zhuang et al., 2018; Singh et al., 2017). Also, information about future solar activity is needed to plan our space missions. Thus, there is a need to predict the peak of the upcoming solar cycles.

Presently, there are many models available in the literature for the prediction of upcoming solar cycle (Pesnell and Schatten, 2018; Bhowmik and Nandy, 2020). Some of them are data-based statistical models (Ohl, 1966; Thompson, 1993; Hathaway, 2015), whereas some models are dynamo-based (Dikpati and Charbonneau, 1999; Macario-Rojas et al., 2018). In precursor-type forecasting models, the information of preceding solar cycles is utilized to predict the peak of the future solar cycle (Svalgaard et al., 2005; Muñoz-Jaramillo et al., 2013; Cameron et al., 2016). Recently, information of planets in our solar system is also being used to understand the variations in the solar cycle. Courtillot et al. (2021) used the astronomical ephemeris from the catalogs of aphelia of the four Jovian planets and suggested that this information can be used to forecast the variations in the solar activity, represented by the sunspot series. On similar lines, it is shown that the most prominent temporal

<sup>\*</sup> Corresponding author.

E-mail addresses: [bharati.kakad@iigm.res.in](mailto:bharati.kakad@iigm.res.in) (B. Kakad), [amar.kakad@iigm.res.in](mailto:amar.kakad@iigm.res.in) (A. Kakad).

<https://doi.org/10.1016/j.pss.2021.105359>

Received 29 June 2021; Received in revised form 7 October 2021; Accepted 9 October 2021

Available online 14 October 2021

0032-0633/© 2021 Elsevier Ltd. All rights reserved.

features of the solar activity can be explained by double synchronization with the 11.07 years periodic tidal forcing of the Venus–Earth–Jupiter system (Stefani et al., 2021). Apart from the uncertainty involved in different methods, in most of the models, the prediction of only one following solar cycle is available at the end of the preceding solar cycle (Kakad, 2011; Kakad et al., 2017b). However, it is preferable to have a prediction of the upcoming solar cycles well in advance. Even if we get some information about the average level of peak solar activity for future solar cycles then it is useful to understand the trend in the upcoming solar cycles. In present study, we have paired two solar cycles starting with even numbered solar cycle. In other words, we are considering the activity for Hale's magnetic solar cycle, which has a period of approximately 22 years. We have estimated the sum of the peak SSN and the lengths associated with each even-odd pair of solar cycle. The present data-based model can predict the sum of peak SSN of upcoming two consecutive solar cycles (i.e., Hale's whole solar cycle) using information of preceding two solar cycles. It implies that the model can provide the peak SSN of  $n + 1$ , and sum of peak SSN of  $n + 2$  and  $n + 3$  solar cycles at the end of each  $n$ th solar cycle. As we have utilized the even-odd pair of solar cycle the  $n$  is allowed to take even-numbered solar cycles (i.e. 2, 4, 6 ... etc).

In the present model, we have utilized both daily and monthly sunspot numbers for solar cycles 10–24 and 2–24, respectively. The data used and the development of the model are described in Section 2 and Section 3, respectively. The prediction of solar cycles 25, 26, and 27 is elaborated in Section 4. The present study is discussed and concluded in Section 5 and Section 6, respectively.

## 2. Data used

Sunspot-number data is the longest available data series, which is often used to develop the prediction models for solar activity. Prior to the year 2014, the sunspot number Version-1 data was accessible (Ohl, 1966; Thompson, 1993; Hathaway, 2015), which recently has been corrected, and available as Version-2 sunspot-number data (Clette et al., 2014, 2016). This newly calibrated sunspot-number series includes several corrections of the past inhomogeneities in the time series and now it is being used to monitor the solar activity. In the present model, we have used both daily and monthly international sunspot number data provided by SIDC SILSO (<http://www.sidc.be/silso/>). The sunspot number follows a cyclic behaviour with an average periodicity of approximately 11 years, known as solar cycle. For a given month the monthly smoothed sunspot number (referred as SSN) is obtained by smoothing of monthly sunspot numbers with a 13-month filter centered on the month of interest with half weights for the months at the start and end (Hathaway, 2010). It is a standard smoothing technique, which is used to get the solar cycle characteristics like peak, start time, length of solar cycle etc. By tracking variation in the monthly smoothed sunspot number and sunspot-less days (i.e., days without sunspot), each  $n$ th solar cycle is characterized by (i) the start time,  $t_s^n$ , defined as the time of occurrence of the minimum in SSN [ $S_{\min}^n$ ], (ii) the peak time,  $t_p^n$  taken as the time of occurrence of the maximum in SSN [ $S_{\max}^n$ ], and (iii) the end time,  $t_e^n$  is same as the start time of solar cycle  $n + 1$ . The length of solar cycle,  $T_{cy}^n$  is given by  $t_e^n - t_s^n$ . All these solar cycle characteristics are available at <http://sidc.be/silso/cyclesminmax> and we have listed these characteristics in Table 1. The daily and monthly sunspot number sunspot data is available for solar cycles 10–24 and solar cycles 1–24, respectively. The daily sunspot-number data has frequent data gaps in solar cycles 6–9 therefore we have used daily sunspot-number data starting from solar cycle 10. The variation of daily and monthly sunspot-number data is plotted as a function of time superimposed with monthly SSN in Fig. 1a and b, respectively. The time of the peak SSN for each solar cycle is marked by the vertical dot-dashed lines. The cyclic behaviour of solar cycles and variation in the peak SSN from one solar cycle to another is clearly evident in Fig. 1. In the next section, we have discussed the development

**Table 1**

Solar cycle characteristics, namely, start time,  $t_s$ , peak time,  $t_p$ , end time,  $t_e$ , length of solar cycle,  $T_{cy}$  peak sunspot number  $S_{\max}$  for the Version-2 sunspot number series. All times are given in years. The area under the solar cycle curve estimated using monthly sunspot number are provided in the last column. It is in the unit of sunspot number-day [SN-day].

SCN	$t_s$ [year]	$t_p$ [year]	$t_e$ [year]	$T_{cy}$	$S_{\max}$	$A_{\text{monthly}}^n$ [SN-day]
1	1755.17	1761.50	1766.50	11.33	144.1	$2.87 \times 10^5$
2	1766.50	1769.75	1775.50	9.00	193	$3.26 \times 10^5$
3	1775.50	1778.42	1784.75	9.25	264.2	$3.75 \times 10^5$
4	1784.75	1788.17	1798.33	13.58	235.3	$5.12 \times 10^5$
5	1798.33	1805.17	1810.58	12.25	82	$1.73 \times 10^5$
6	1810.58	1816.42	1823.42	12.83	81.2	$1.43 \times 10^5$
7	1823.42	1829.92	1833.92	10.50	119.2	$2.42 \times 10^5$
8	1833.92	1837.25	1843.58	9.67	244.9	$3.96 \times 10^5$
9	1843.58	1848.17	1856.00	12.42	219.9	$4.51 \times 10^5$
10	1856.00	1860.17	1867.25	11.25	186.2	$3.79 \times 10^5$
11	1867.25	1870.67	1879.00	11.75	234	$3.81 \times 10^5$
12	1879.00	1884.00	1890.25	11.25	124.4	$2.33 \times 10^5$
13	1890.25	1894.08	1902.08	11.83	146.5	$2.81 \times 10^5$
14	1902.08	1906.17	1913.58	11.50	107.1	$2.26 \times 10^5$
15	1913.58	1917.67	1923.67	10.08	175.7	$2.70 \times 10^5$
16	1923.67	1928.33	1933.75	10.08	130.2	$2.51 \times 10^5$
17	1933.75	1937.33	1944.17	10.42	198.6	$3.65 \times 10^5$
18	1944.17	1947.42	1954.33	10.17	218.7	$4.04 \times 10^5$
19	1954.33	1958.25	1964.83	10.50	285	$4.95 \times 10^5$
20	1964.83	1968.92	1976.25	11.42	156.6	$3.63 \times 10^5$
21	1976.25	1980.00	1986.75	10.50	232.9	$4.26 \times 10^5$
22	1986.75	1989.92	1996.67	9.92	212.5	$3.85 \times 10^5$
23	1996.67	2001.92	2009.00	12.33	180.3	$3.71 \times 10^5$
24	2009.00	2014.33	2019.95	11.0	116.4	$1.99 \times 10^5$

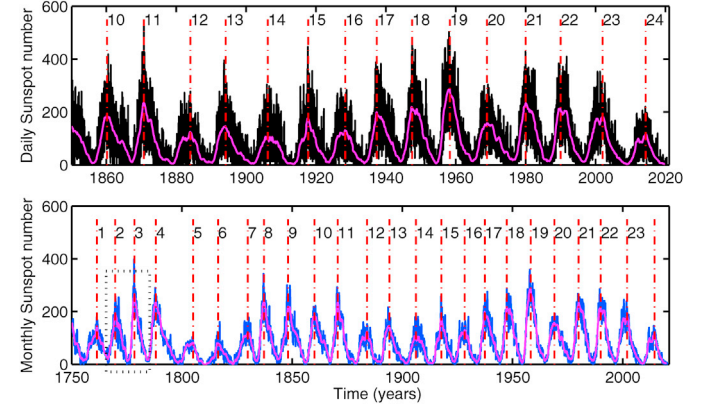


**Fig. 1.** Variation of daily sunspot number (upper panel) and monthly sunspot number (lower panel) data as a function of time with superimposed monthly smoothed sunspot number (magenta color). The time of the peak SSN for each solar cycle is marked by the vertical dot-dashed lines. One of the even-odd pair of solar cycle is marked with the black rectangle in lower panel.

of the prediction model.

## 3. Development of model

In this model, we have utilized the information of the area under the curve of each solar cycle, and its length, and peak (or amplitude). For each  $n$ th solar cycle we have estimated the area under the curve [ $A^n$ ] by considering the sunspot number variations from start time  $t_s^n$  up to the end time  $t_e^n$ . These estimates are separately obtained from daily and monthly sunspot numbers for solar cycles 10–24 and 1–24 solar cycles, respectively. For each  $n$ th solar cycle the area under the curve of the solar cycles is calculated using  $A^n = \int_{t_s^n}^{t_e^n} s \times dt$ , where  $dt$  is time resolution of sunspot data expressed in units of day and  $s$  is daily or monthly sunspot number. The area under the curve of solar cycles estimated using daily sunspot numbers ( $s_d$ ) and monthly sunspot numbers ( $s_m$ ) are shown in

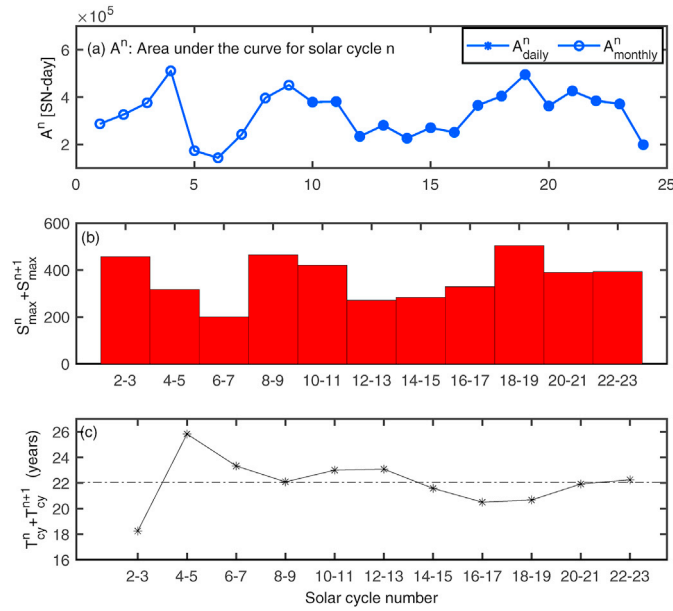


**Fig. 2.** (a) The area under the curve of solar cycle estimated from daily sunspot number (for solar cycles 10–24) and monthly sunspot number (for solar cycles 1–24) as a function of solar cycle number (SCN). Sum of the (b) peak SSN, and (c) length for even-odd pair of solar cycles (eg. solar cycles 2–3, 4–5, 6–7, up to 22–23) are shown as a function of solar cycle number. The average value of length of pair of even-odd solar cycle is shown by horizontal dashed-dotted line in panel (c).

**Fig. 2(a)** for solar cycles 10–24 and solar cycles 1–24, respectively. The estimates of area under the curve of solar cycle are in the range of  $1.43 \times 10^5 - 5.12 \times 10^5$  for solar cycles 1–24. Sunspot numbers are mere counts and do not have any physical unit, therefore the area under the curve of solar cycle is expressed in units of sunspot number-day (i.e., SN-day). It may be noted that as daily sunspot-number data has a higher time resolution as compared to monthly sunspot-number data, the estimates of  $A^n$  obtained from daily and monthly sunspot numbers for a given solar cycle may vary. The monthly sunspot number,  $s_m$  is average of the daily sunspot number for a given month. Daily sunspot number varies from day-to-day, and for a given month these variations can be quantified using standard deviation  $\sigma$  in  $s_m$ . It may be noted that average  $\sigma$  varies in the range of 0–150 with  $\langle\sigma\rangle \sim 30$ . In other words, the upper and lower boundary for the daily sunspot number variations can be considered as  $s_m \pm \sigma$ . As this standard deviation is small, even for one solar cycle (around 132 months) the area under the curve of solar cycle computed from daily and monthly sunspot numbers,  $|A_{\text{daily}}^n - A_{\text{monthly}}^n|$ , for solar cycles 10–24 is considerably small ( $\approx 31$ –721). Therefore there is a good match in the variation of  $A^n$  estimated from daily and monthly sunspot-number data as evident in **Fig. 2(a)**. The values of area under the curve of solar cycle estimated from monthly sunspot numbers are given in **Table 1**.

Although we observe a periodicity of approximately 11 years in sunspot number, the magnetic cycle of the Sun has an average periodicity of approximately 22 years, which is widely known as Hale's magnetic solar cycle (Hale et al., 1919). While developing the present prediction model, first, we have clubbed the information of two solar cycles together starting from even-numbered solar cycles. For example, we paired solar cycles 2–3, 4–5, 6–7, up to 22–23 together and estimated the sum of their peak SSN and length, which is shown in **Fig. 2(b)** and (c), respectively. The values of summation of peak SSN and length for solar cycle pair  $n$  and  $n + 1$  are in the range of  $\Sigma_{n+1}^{n+1} S_{\text{max}} \approx 200.4$ –503.7 and  $\Sigma_{n+1}^{n+1} T_{\text{cy}} \approx 18.3$ –25.8 years, respectively. The average value of  $\Sigma_{n+1}^{n+1} T_{\text{cy}}$  is  $22.1 \pm 1.9$  years, which is depicted by horizontal dashed-dot line in **Fig. 2(c)**. The lower limit of  $\Sigma_{n+1}^{n+1} S_{\text{max}}$  of 200.4 is associated with solar cycles 6–7, which falls under the Dalton minimum. Whereas, the higher limit of  $\Sigma_{n+1}^{n+1} S_{\text{max}}$  of

503.7 is associated with solar cycles 18–19, which falls under the modern maxima. In **Fig. 3**, we have plotted the area under the curve of solar cycle estimated from daily (red color) and monthly (blue color) sunspot-number data as a function of peak SSN for solar cycles 10–24 and 1–24, respectively. It is evident that the area under the curve of solar cycle is directly proportional to the peak SSN and possesses a correlation coefficient of 0.91, which has statistical significance above 95%. We have fitted a straight line to this variation using the least square method, which gives the following equation (1),

$$A^n = 1830.7 \times S_{\text{max}}^n \quad (1)$$

In above equation (1) the coefficient of the linear fit has an error of  $\pm 67$ . It is evident from **Fig. 3** that area under the curve of solar cycle is directly proportional to its peak SSN. Such a tendency is expected and can be understood in the light of the functions used to fit the shape of the solar cycle. To fit the time variation of sunspot number in a given solar cycle Hathaway (2015) has given an analytical form  $F(t)$ , which is a combination of the fixed cubic power law and a Gaussian function. In this analytical function one of the parameter is amplitude that decides the peak SSN in the fitted curve  $F(t)$ . Therefore, if we integrate  $F(t)$ , which is similar to the area under the curve then it is proportional to the amplitude of the solar cycle. Equation (1) can be used to get the provisional estimates of the area under the curve of a solar cycle with the knowledge of peak SSN ( $S_{\text{max}}$ ). We have used this equation (1) to get the area of future solar cycle 25, which is explained later in Section 4. While examining the variation of  $A^n$ , we noted that difference in the area under the curve of solar cycle  $n$  and  $n + 1$  can be used in the model to get the summation of peak SSN of  $n + 2$  and  $n + 3$  solar cycles. Here,  $n$  is allowed to take only even numbers (i.e., 2, 4, 6 ... 22 etc.). In the model, we have considered one parameter as  $Y = [S_{\text{max}}^{n+2} + S_{\text{max}}^{n+3}]$  and other parameter as  $X = [A^n - A^{n+1}] / [T_{\text{cy}}^n + T_{\text{cy}}^{n+1}]$ . We have plotted the model parameter  $Y$  as a function of  $X$  for solar cycles 10–22 using daily sunspot-number data in **Fig. 4(a)** and for solar cycles 2–22 using monthly sunspot-number data in **Fig. 4(b)**. As we have utilized daily sunspot-number data for solar cycles 10–24 in **Fig. 4(a)**, and monthly sunspot-number data for solar cycles 2–24 in **Fig. 4(b)** we have total 6 and 10 points in respective figures. We find that the correlation coefficient between model parameters  $X$  and  $Y$  are 0.92 and 0.85, which is based on the daily and monthly sunspot-number data, respectively.

These correlations are based on total 6 and 9 number of data points, respectively and satisfy the statistical significance of 95%. It may be

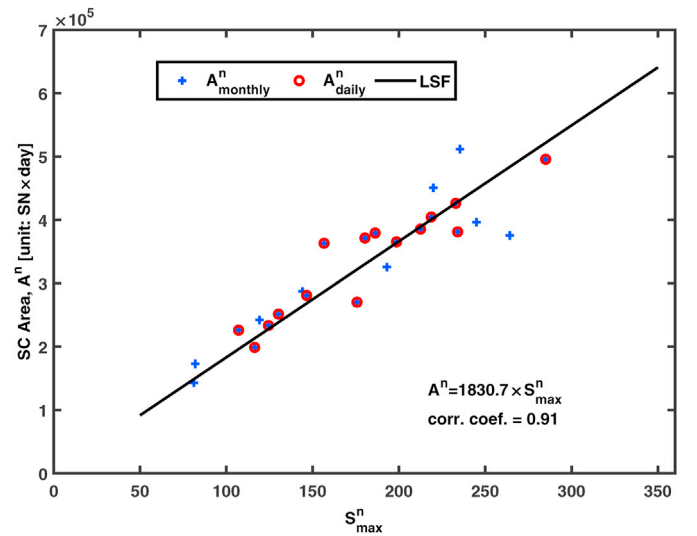


**Fig. 3.** Area under the curve of solar cycle computed from daily (red) and monthly (blue) sunspot number as a function of peak SSN for solar cycles 10–24 and 1–24, respectively.

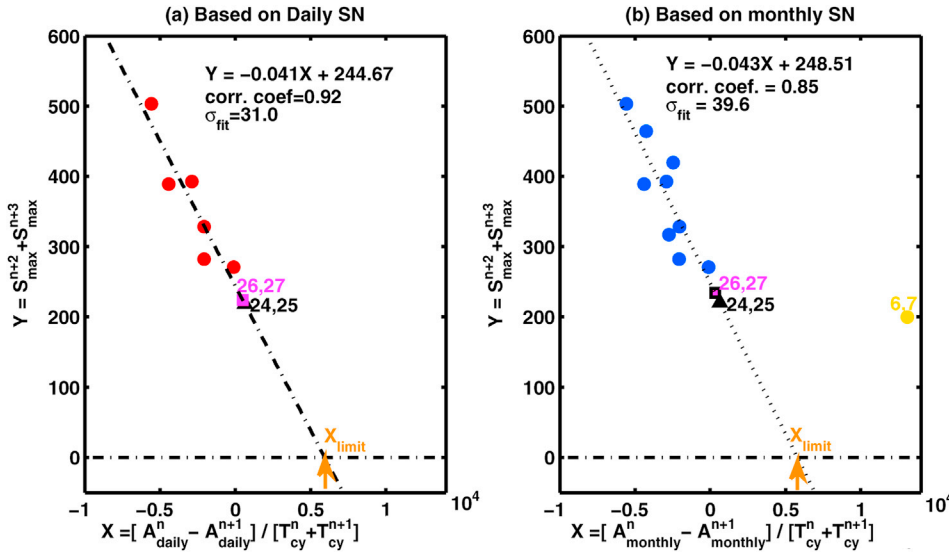


Fig. 4. Model parameters,  $Y = [S_{\max}^{n+2} + S_{\max}^{n+3}]$  as a function of  $X = [A^n - A^{n+1}] / [T_{\text{cy}}^n + T_{\text{cy}}^{n+1}]$  for (a) solar cycles 10–22 using daily sunspot-number data, and (b) solar cycles 2–22 using monthly sunspot-number data. Here,  $n$  is allowed to take only even-numbered solar cycles. The predicted summation of peak SSN for solar cycles 24–25 and solar cycles 26–27 are marked by black and magenta color, respectively. The least square first order fit equation is given in respective subplots. The upper limiting value of  $X_{\text{limit}}$  in the respective case is marked by an arrow and it represents the  $X$  parameter beyond which the corresponding model equation is not applicable.

noted that one data point (shown by yellow circle) appears as distinct outlier in Fig. 4(b). This point is associated with solar cycle pair 6–7 (i.e.,  $n + 2 = 6$  and  $n + 3 = 7$ ) and it is not considered while computing the correlations. We have fitted a straight line to variation of  $X$  and  $Y$  using least squares fit, which gives the following equation (2) using daily sunspot number, and equation (3) using monthly sunspot number.

$$S_{\max}^{n+2} + S_{\max}^{n+3} = a_1 \times \frac{[A_{\text{daily}}^n - A_{\text{daily}}^{n+1}]}{[T_{\text{cy}}^n + T_{\text{cy}}^{n+1}]} + a_0 \quad (2)$$

$$S_{\max}^{n+2} + S_{\max}^{n+3} = b_1 \times \frac{[A_{\text{monthly}}^n - A_{\text{monthly}}^{n+1}]}{[T_{\text{cy}}^n + T_{\text{cy}}^{n+1}]} + b_0 \quad (3)$$

In equation (2) there are two coefficients, which are  $a_1 = -0.041 \pm 0.008$  and  $a_0 = 244.7 \pm 29.5$ . Similarly, in equation (3) there are two coefficients that are  $b_1 = -0.043 \pm 0.007$  and  $b_0 = 248.5 \pm 23.3$ . Here,  $A_{\text{daily}}^n$  and  $A_{\text{monthly}}^n$  are the area under the curve of the solar cycle  $n$  obtained from the daily and monthly sunspot number, respectively. It may be noted that coefficients appearing in equations (2) and (3) are similar (i.e.,  $a_1 \approx b_1$  and  $a_0 \approx b_0$ ) and it implies that we can use any of the equation to get the prediction of  $S_{\max}^{n+2} + S_{\max}^{n+3}$  by utilizing the length and the area under the curve of preceding solar cycles  $n$  and  $n + 1$ . Here, the coefficient  $a_1$  and  $b_1$  are negative, which indicates that as the difference in the area under the curve of  $n$  and  $n + 1$  solar cycle decreases the summation of the peak SSN of upcoming  $n + 2$  and  $n + 3$  is likely to increase. Another important feature of the model equations (2) and (3) is that there exist an upper threshold on the value of  $A^n - A^{n+1}$ . If we assume no solar activity for upcoming solar cycles i.e.,  $Y = S_{\max}^{n+2} + S_{\max}^{n+3} = 0$  then the limiting value  $X_{\text{limit}} = -a_0/a_1$  from equation (2) comes out to be 5968. Similarly, from equation (3) we get  $X_{\text{limit}} = -b_0/b_1$  as 5779. These values of  $X_{\text{limit}}$  are marked in Fig. 4(a) and (b). On an average  $\langle X_{\text{limit}} \rangle$  is 5873. This limiting value of parameter  $X$  enforces an upper limit of  $1.30 \times 10^5$  on  $A^n - A^{n+1}$ . In this calculation, while computing  $A^n - A^{n+1}$  from  $\langle X_{\text{limit}} \rangle$ , we took average value of  $\langle T_{\text{cy}}^n + T_{\text{cy}}^{n+1} \rangle$  as approximately  $22.1 \pm 1.9$  years. It suggests that if the difference in the area under the curve of the solar cycle  $n$  and  $n + 1$  is less than the limiting value of  $[A^n - A^{n+1}]_{\text{limit}} = 1.30 \times 10^5$  then only we can use above model equations (2) and (3) to predict  $S_{\max}^{n+2} + S_{\max}^{n+3}$ .

The conditions for which  $[A^n - A^{n+1}]$  exceeds  $1.30 \times 10^5$  the  $S_{\max}^{n+2} + S_{\max}^{n+3}$  becomes negative, which is physically unreliable and in such scenario the present model is not applicable. The question is whether we have encountered  $[A^n - A^{n+1}] > 1.30 \times 10^5$  for solar cycles 1–24? The

answer is yes, we have met such situation for solar cycle 4 and 5 (i.e.,  $n = 4$ ,  $n + 1 = 5$ ). The value of  $A^4 - A^5 = 3.39 \times 10^5$ , which is much larger than the limiting value of  $[A^n - A^{n+1}]_{\text{limit}}$  and the corresponding value of associated upcoming peak SSN is  $S_{\max}^{n+2} + S_{\max}^{n+3} = 248.5$ . This particular data point is shown by yellow circle in Fig. 4(b) and it is basically an outlier. It may be noted that we have excluded this outlier point while estimating the model equation (3). Therefore it is obvious that this outlier data point will not follow the limits enforced by the model equation on  $[A^n - A^{n+1}]$ . Interestingly, this outlier point is associated with significantly weak activity period of solar cycles 5–7, which is known as the period of Dalton minimum. The peculiar behaviour of this outlier point is checked in view of Gnevyshev-Ohl rule and discussed in Section 5. The present model can be used to get the prediction of  $S_{\max}^{n+2} + S_{\max}^{n+3}$  only if the estimates of  $[A^n - A^{n+1}] < 1.30 \times 10^5$ . For the cases, where  $[A^n - A^{n+1}] > 1.30 \times 10^5$  the solar cycles  $n + 2$  and  $n + 3$  may experience weaker solar activity as encountered in the period of Dalton minimum. The r.m.s. error  $\sigma_{\text{fit}}$  in the observed and predicted values of peak SSN  $S_{\max}^{n+2} + S_{\max}^{n+3}$  for  $n = 2, 4, 6, \dots, 22$  using model equations (2) and (3) are 31 and 39.6, respectively, and it is considered as the possible error in the prediction of  $S_{\max}^{n+2} + S_{\max}^{n+3}$  obtained using the present model.

Now let us talk about the error in the prediction. The mean of 1–23 solar cycle,  $\langle S_{\max} \rangle = 114.1 \pm 40.4$  and it is based of Version-1 sunspot number. This average amplitude provides the benchmark for the prediction models. In other words, it is a simple prediction without any skills, therefore any prediction models must have better accuracy than this standard error (Hathaway, 2015). It may be noted that for Version-2 sunspot number the average of peak SSN for 1–24 solar cycle comes out to be  $\langle S_{\max} \rangle = 178.7 \pm 57$ . In our model the expected error in  $S_{\max}^{n+2} + S_{\max}^{n+3}$  is around  $\pm 31.0$  but it is the error in the sum of peak of two solar cycles and not the  $S_{\max}$  of a single solar cycle. If we give equal weight to the standard error then the error in the prediction of  $S_{\max}^{n+2}$  and  $S_{\max}^{n+3}$  will be approximately 15. On the other hand, if we provide correct value of the  $S_{\max}^{n+2}$ , it means we are certain about the peak of  $n + 2$  solar cycle then the error in the forecast of  $S_{\max}^{n+3}$  will be approximately 31. Therefore, one can say that in present model the error in the prediction of  $S_{\max}$  is 15–31, which is well within the significance limit proposed by (Hathaway, 2015). The prediction of peak SSN for solar cycles 25, 26 and 27 is briefed in the next Section.

#### 4. Prediction of solar cycle 25, 26 and 27

As mentioned earlier, the coefficients in the model equations (2) and



(3) are similar. Thus, we can use either of the equation to predict the peak SSN of the upcoming two solar cycles. The similarity in the model equations (2) and (3) is obvious because the estimates of the area under the curve of solar cycle estimated using the daily and monthly sunspot numbers differ less significantly. Here, we have used equation (2) to get the predictions of solar cycles 24–25 and solar cycles 26–27. As the current solar cycle 24 has approached its end and solar cycle 25 has initiated from December 2019, we can estimate the area under the curve of solar cycle 24 i.e.,  $A^{24}$ . We took  $T_{cy}^{24} = 11.0$  years. Recently, the solar cycle 25 prediction panel have declared that the solar cycle 24 ended in December 2019 and new solar cycle 25 has commenced (<https://www.weather.gov/news/201509-solar-cycle>). We took  $n = 22$ ,  $n + 1 = 23$  and utilized estimates of  $A^{22} = 3.85 \times 10^5$ ,  $A^{23} = 3.71 \times 10^5$ ,  $T_{cy}^{22} = 9.92$ ,  $T_{cy}^{23} = 12.33$  in equation (2), which gives  $S_{max}^{24} + S_{max}^{25}$  as 218.7. We know that  $S_{max}^{24}$  is 116.4 therefore the peak SSN of solar cycle 25 comes out to be 102.3. After getting the prediction for  $S_{max}^{25}$ , we estimated the area under the curve of solar cycle 25 by using equation (1). By considering the possible error in the coefficient of equation (1) we get  $A^{25}$  in the range of  $1.80 \times 10^5$  to  $1.94 \times 10^5$ . Now for solar cycle 25, we have prediction of the peak SSN and subsequently the speculated estimates of the area under the sunspot number curve. Therefore, we took  $n = 24$ ,  $n + 1 = 25$  and utilized estimates of  $A^{24} = 1.99 \times 10^5$ ,  $A^{25} = 1.87 \pm 0.06 \times 10^5$ ,  $T_{cy}^{24} = 11.0$ , and  $T_{cy}^{25} = 12.2$  in equation (2) which yields  $S_{max}^{26} + S_{max}^{27}$  as 212–236. It may be noted that length of solar cycle 25 ( $T_{cy}^{25}$ ) is taken from the model by Kakad et al. (2017a). Using model equation (2) the predicted value of  $S_{max}^{25}$  and  $S_{max}^{27}$  comes out to be 218.7 and 224.2, respectively. These predicted summation of peak SSN of pair of solar cycles are depicted by black triangle and magenta square in Fig. 4(a) and (b), respectively and it implies that the peak SSN of solar cycle 26 and 27 might be similar or slightly stronger than solar cycle 24 and 25. It may be noted that the present model forecasts the summation of peak SSN of upcoming two solar cycles (i.e.,  $n + 2$  and  $n + 3$ ) using information of preceding two solar cycles (i.e.,  $n$  and  $n + 1$ ).

Using present model we forecast  $S_{max}^{25} = 102.3 \pm 15$ , which indicate that solar cycle 25 could be slightly weaker ( $\approx 12\%$ ) than the solar cycle 24. Some other model predictions of peak SSN of solar cycle 25 lies in the close range of 110–125 (Bhowmik and Nandy, 2018; Jiang et al., 2018; Upton and Hathaway, 2018). Whereas, the flux transport dynamo model indicate that the solar cycle 25 would be weaker than solar cycle 24 with peak SSN as 89 (Labonville et al., 2019). In addition, some other models forecast slightly stronger solar cycle 25 with peak SSN in the range of 130–144 (Pesnell and Schatten, 2018; Kakad et al., 2020). The international panel to forecast Solar Cycle 25 gave their latest forecast for Solar Cycle 25 as 115. The panel agreed that the solar cycle 25 would be average in intensity and similar to solar cycle 24 (see <https://www.swpc.noaa.gov/news>).

## 5. Discussion

In the present model, we have clubbed two solar cycles together in such a way that it starts from even solar cycle (i.e.,  $n = 2, 4, 6, \dots, 24$ ), which implies an even-odd pair of solar cycles in sequence and estimated sum of their peak SSN, and total length (see Fig. 2b and c). By utilizing this information, we could develop a model that forecast the sum of the peak SSN of solar cycle  $n + 2$  and  $n + 3$ . This model provides good correlation for the model parameters  $X$  and  $Y$  (See Fig. 4). However, the solar cycles are paired using “even-odd” cycles, i.e., in this model  $n$  is allowed to take even number. Obvious question is what happens if we pair solar cycles using “odd-even” pair of solar cycle. If we club two solar cycles starting from the odd solar cycle (i.e.,  $n = 1, 3, 7, \dots, 23$ ) then the present model is not valid as the correlation coefficient between the model parameters  $Y$  and  $X$  decreases considerably and it is not statistically significant. The relation of model parameters,  $Y$  as a function of  $X$  for odd-even solar cycle pairs is given in Fig. 6. It is observed that if we

incorporate the odd-even pair of solar cycles then the model parameters  $X$  and  $Y$  are poorly correlated and there are three data points that appears as outlier, which are associated with solar cycles 5–6, 9–10, and 21–22. Therefore, we can say that the present model works well with the even-odd pair of solar cycles and not with the odd-even pair of solar cycle. This tendency raises a question that why the model is sensitive to a choice of even-odd pair of solar cycle. Probably reason for such peculiar dependence on the pairing of solar cycles could be related to the Gnevyshev-Ohl rule, which is also widely known as odd-even effect. Gnevyshev and Ohl (1948) showed that the even-numbered solar cycle is followed by higher amplitude odd-numbered solar cycle. This tendency in variation in the sunspot number is known as the Gnevyshev-Ohl rule. In general, it can be verified in different ways for example (i) the peak SSN of even-numbered solar cycle is less than the following odd-numbered solar cycle, (ii) the sum of sunspot number of even-numbered solar cycle is less than the following odd-numbered solar cycle and (iii) the area under the curve of sunspot number cycle of even-numbered solar cycle is less than the following odd-numbered solar cycle (Kopecký, 1950; Hathaway et al., 2002; Tlatov, 2013). This rule suggests that the fundamental cycle of the Sun (Hale magnetic cycle, 22 years) consists of two solar cycles starting from even-numbered solar cycles. We utilized the area under the curve of the solar cycle to check this dependence. In Fig. 5(a) the area under the curve of sunspot number for even-numbered solar cycle is plotted as a function of odd-numbered solar cycle, and their respective ratios  $A_{odd}^{n+1}/A_{even}^n$  are shown in Fig. 5(b) for solar cycles 2–24. Here,  $n$  represents even-numbered solar cycle such that  $n = 2, 4, 6, \dots, 22$ . It is noted that the  $A_{odd}^{n+1}$  vary directly with  $A_{even}^n$  with correlation coefficient of 0.90, and their dependence is given by following equation,

$$A_{odd}^{n+1} = 0.80 A_{even}^n + 1.16 \times 10^5 \quad (4)$$

The ratio of area under the curve of solar cycle 24 and 25 is also marked with a black triangle in Fig. 5(b). It may be noted that even-odd pair of solar cycle 4–5 appears as the outlier in Fig. 5(b) and it is shown by yellow solid square. Its behaviour is different as compared to other even-odd solar cycles and it is evident in Fig. 5(b) as well. The ratio of area under the curve of solar cycle,  $A_{odd}^{n+1}/A_{even}^n \geq 1$  for all even-odd pair of solar cycles except the solar cycle 4–5 and these two solar cycles falls in the period of the Dalton minimum. Tlatov (2013) had reported that the ratio of  $A_{odd}^{n+1}/A_{even}^n$  has a long-term variation ranging between 0.5 and 1.5 with

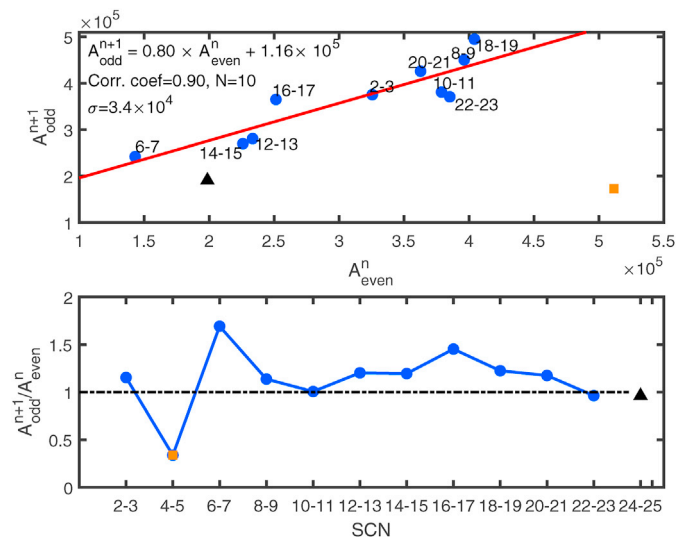
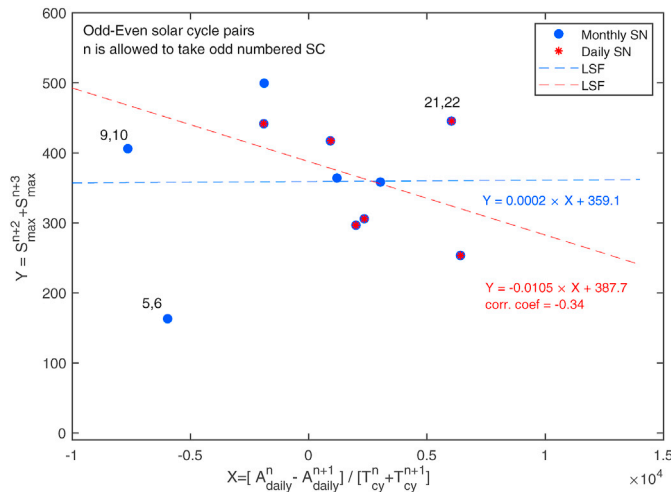


Fig. 5. (a) The area under the curve of solar cycle for odd-numbered solar cycle [ $A_{odd}^{n+1}$ ] as a function of even-numbered solar cycle [ $A_{even}^n$ ]. (b) The ratio of area under the curve of solar cycle with odd-numbered solar cycle to that of even-numbered solar cycle as a function of pair of even-odd solar cycles.



**Fig. 6.** Model parameters,  $Y = S_{\max}^{n+2} + S_{\max}^{n+3}$  as a function of  $X = [A^n - A^{n+1}] / [T_{\text{cy}}^n + T_{\text{cy}}^{n+1}]$  for solar cycles 1–23 using monthly sunspot-number data. Here,  $n$  is allowed to take only odd-numbered solar cycles.

a period of about 21 solar cycles, and it is related to the reversal of the Gnevyshev-Ohl rule. During such reversals the ratio of  $A_{\text{odd}}^{n+1} / A_{\text{even}}^n < 1$  which is similar to that as encountered during solar cycles 4–5. The solar cycle pair 4–5 do not follow Gnevyshev-Ohl rule and for this case the associated data point appears as an outlier in Fig. 4b. The point is so distinct from the set of other data points (where Gnevyshev-Ohl rule is satisfied) that even with least absolute deviation fitting method the error in observed and fitted value of  $Y$  is very large. Therefore, we have ignored this point while computing the model equation (3). Thus, it is clear that the proposed prediction model is applicable to the even-odd pair of solar cycles that are following Gnevyshev-Ohl rule i.e.,  $A_{\text{odd}}^{n+1} / A_{\text{even}}^n \geq 1$ . We know that the solar cycle variations as recorded in sunspot number is a result of the solar dynamo, which is highly nonlinear and complex process. It is demonstrated that the Gnevyshev-Ohl rule can be reproduced well through mean-field dynamo model, which is based on a realistic rotation profile and on nonlinearity that is associated with the magnetic helicity balance (Pipin et al., 2012). These authors noticed that lower helicity dissipation rate help in maintaining the correlation between solar cycles (eg. Gnevyshev-Ohl rule and Waldmeier Effect). The proposed model equations (2) and (3) can be used to predict the peak SSN of  $n + 1$  and summation of peak SSN of  $n + 2$  and  $n + 3$  at the end of  $n$ th solar cycle, provided  $n$  is even-numbered solar cycle.

## 6. Summary and conclusions

A new prediction model of peak sunspot number is presented. This model can provide information about the peak SSN of the upcoming solar cycle  $n + 1$ , and summation of peak SSN of solar cycle  $n + 2$ , and  $n + 3$  at the end of each even-numbered  $n$ th solar cycle. For example presently, we are at the end of solar cycle 24, so we can forecast the peak SSN for solar cycles 25 and summation of peak SSN of 26 and 27. equations (2) and (3) are the prediction equations, which are obtained using daily and monthly sunspot-number data of solar cycles 10–23 and 2–23, respectively. One can use either of the equations for the forecasting. In this model, we utilized, the area under the sunspot-number curve of solar cycle  $n$  and  $n + 1$  and their respective lengths to get the estimates of summation of peak SSN of  $n + 2$  and  $n + 3$  solar cycles,  $[S_{\max}^{n+2} + S_{\max}^{n+3}]$ . Here,  $n$  is allowed to take only even-numbered solar cycles. In other words, the model is applicable only for the even-odd pair of solar cycles. If we consider odd-even pair of solar cycle then this model is not suitable for the prediction. This peculiar dependence of this model on choice of

even-odd solar cycles is attributed to the Gnevyshev-Ohl rule (Gnevyshev and Ohl, 1948). We find that the proposed prediction model is applicable to the even-odd pair of solar cycles that are following Gnevyshev-Ohl rule i.e.,  $A_{\text{odd}}^{n+1} / A_{\text{even}}^n \geq 1$ . Such even-odd pair of solar cycles together forms the Hale's magnetic solar cycle of approximately 22 years. This cycle to cycle correlation supported by Gnevyshev-Ohl rule is successfully demonstrated by the mean-field dynamo model by lowering the helicity dissipation rate (Pipin et al., 2012). The model equation has two parameters, namely,  $Y = [S_{\max}^{n+2} + S_{\max}^{n+3}]$  and  $X = [A^n - A^{n+1}] / [T_{\text{cy}}^n + T_{\text{cy}}^{n+1}]$ , which are in good correlation ( $\geq 0.85$ ). We found that as the difference in the area of  $n$  and  $n + 1$  solar cycle decreases the summation of peak SSN of upcoming  $n + 2$  and  $n + 3$  is likely to increase. Generally, we are interested in the forecast of peak of a single solar cycle rather than the sum of two consecutive solar cycles. In our model we are forecasting sum of peak SSN of two consecutive upcoming solar cycles (i.e.,  $S_{\max}^{n+2} + S_{\max}^{n+3}$ ) using even-odd pair of solar cycle  $n$  and  $n + 1$ . However, sum of two solar cycles also give us clue about the trend in the upcoming solar cycles. Moreover, if we provide the  $S_{\max}^{n+2}$  then one can get the information about the  $S_{\max}^{n+3}$  in advance and this prediction will be available after the time of the peak SSN of solar cycle  $n + 2$ .

Our model predicts the peak SSN of solar cycle 25 as  $S_{\max}^{25} = 103 \pm 15$ . Further, it predicts that the  $S_{\max}^{26} + S_{\max}^{27} = 229.4 \pm 31$ . For solar cycle 24 and 25 the predicted  $S_{\max}^{24} + S_{\max}^{25} = 218.7$  thus, one can say that the solar cycle 26 and 27 might be similar or slightly stronger than solar cycle 24 and 25. We do not have predictions for individual solar cycle 26 and 27 but we can forecast the summation of peak SSN of solar cycle 26 and 27. It gives some information about the average level of solar activity for upcoming solar cycle 26–27. Our predictions are in general agreement with recent study by Javaraiah (2017), where it is suggested that (i) solar cycle 25 will be weaker than solar cycle 24, (ii) solar cycle 25 and 26 will have almost similar strength, and (iii) solar cycle 27 will be stronger than solar cycle 26. For solar cycle 25, our results are in good agreement with some recent studies, which forecast that the upcoming solar cycle 25 will be slightly weaker than solar cycle 24 (Gkana and Zachilas, 2016; Upton and Hathaway, 2018). Some other studies suggest that solar cycle 25 will be similar or slightly stronger than solar cycle 24 (Sarp et al., 2018; Pesnell and Schatten, 2018; Helal and Galal, 2013). For example (Bhowmik and Nandy, 2018), has given a prediction of peak SSN of solar cycle 25 in the range of 109–139. Du (2020) predict peak amplitude of solar cycle 25 as  $137.8 \pm 31.3$  around October 2024, which is higher compared to our forecast of  $S_{\max}^{25} = 103 \pm 15$ . Recent work (Kakad et al., 2020) suggested that solar cycle 25 will be slightly stronger than solar cycle 24. In general, the present model will be useful to get the average level of solar activity during solar cycle 25–27.

## CRedit author statement

Bharati kakad:, Writing- Original draft preparation, methodology. Amar Kakad:. Visualization, Investigation, Reviewing and Editing.

## Declaration of competing interest

The authors declare that they have no known competing financial interests or personal relationships that could have appeared to influence the work reported in this paper.

## Acknowledgement

We thank the SIDC and SILSO teams for the daily and monthly international sunspot data and solar cycle characteristics. We thank reviewers for their valuable comments on the manuscript. The authors declare that they have no conflicts of interest.

## References

- Acero, F., Vaquero, J., Gallego, M., García, J., 2018. A limit for the values of the dst geomagnetic index. *Geophys. Res. Lett.* 45 (18), 9435–9440.
- Alves, M., Echer, E., Gonzalez, W., 2006. Geoeffectiveness of corotating interaction regions as measured by dst index. *J. Geophys. Res.: Space Phys.* 111 (A7).
- Bhowmik, P., Nandy, D., 2018. Prediction of the strength and timing of sunspot cycle 25 reveal decadal-scale space environmental conditions. *Nat. Commun.* 9 (1), 1–10.
- Bhowmik, P., Nandy, D., 2020. Progress in Solar Cycle Predictions: Sunspot Cycles 24-25 in Perspective. URL arXiv:2009.01908.
- Cameron, R.H., Jiang, J., Schuessler, M., 2016. Solar cycle 25: another moderate cycle? *Astrophys. J. Lett.* 823 (2), L22.
- Clette, F., Cliver, E., Lefèvre, L., Svalgaard, L., Vaquero, J., Leibacher, J., 2016. Preface to topical issue: recalibration of the sunspot number. *Sol. Phys.* 291 (9–10), 2479–2486.
- Clette, F., Svalgaard, L., Vaquero, J.M., Cliver, E.W., 2014. Revisiting the sunspot number. *Space Sci. Rev.* 186 (1–4), 35–103.
- Courillot, V., Lopes, F., Le Mouél, J., 2021. On the prediction of solar cycles. *Sol. Phys.* 296 (1), 1–23.
- Dikpati, M., Charbonneau, P., 1999. A babcock-leighton flux transport dynamo with solar-like differential rotation. *Astrophys. J.* 518 (1), 508.
- Du, Z., 2020. Predicting the shape of solar cycle 25 using a similar-cycle method. *Sol. Phys.* 295 (10), 1–11.
- Gkana, A., Zachilas, L., 2016. Re-evaluation of predictive models in light of new data: sunspot number version 2.0. *Sol. Phys.* 291 (8), 2457–2472.
- Gnevyshev, M., Ohl, A., 1948. On the 22-year cycle of solar activity. *Astron. Z.* 25 (1), 18.
- Hale, G.E., Ellerman, F., Nicholson, S.B., Joy, A.H., 1919. The magnetic polarity of sunspots. *Astrophys. J.* 49, 153.
- Hathaway, D.H., 2010. The solar cycle. *Living Rev. Sol. Phys.* 7 (1).
- Hathaway, D.H., 2015. The solar cycle. *Living Rev. Sol. Phys.* 12 (1), 4.
- Hathaway, D.H., Wilson, R.M., Reichmann, E.J., 2002. Group sunspot numbers: sunspot cycle characteristics. *Sol. Phys.* 211 (1–2), 357–370.
- Helal, H.R., Galal, A., 2013. An early prediction of the maximum amplitude of the solar cycle 25. *J. Adv. Res.* 4 (3), 275–278.
- Ingale, M., Janardhan, P., Bisoi, S., 2019. Beyond the mini-solar maximum of solar cycle 24: declining solar magnetic fields and the response of the terrestrial magnetosphere. *J. Geophys. Res.: Space Phys.* 124 (8), 6363–6383. <https://doi.org/10.1029/2019JA026616>.
- Javaraiah, J., 2017. Will solar cycles 25 and 26 be weaker than cycle 24? *Sol. Phys.* 292 (11), 172.
- Jiang, J., Wang, J.-X., Jiao, Q.-R., Cao, J.-B., 2018. Predictability of the solar cycle over one cycle. *Astrophys. J.* 863 (2), 159.
- Kakad, B., 2011. A new method for prediction of peak sunspot number and ascent time of the solar cycle. *Sol. Phys.* 270 (1), 393–406.
- Kakad, B., Kakad, A., Ramesh, D.S., 2017a. Prediction of the length of upcoming solar cycles. *Sol. Phys.* 292 (12), 181.
- Kakad, B., Kakad, A., Ramesh, D.S., 2017b. Shannon entropy-based prediction of solar cycle 25. *Sol. Phys.* 292 (7), 95.
- Kakad, B., Kakad, A., Ramesh, D.S., Lakhina, G.S., 2019. Diminishing activity of recent solar cycles (22–24) and their impact on geospace. *J. Space Weather Space Clim.* 9, A01.
- Kakad, B., Kumar, R., Kakad, A., 2020. Randomness in sunspot number: a clue to predict solar cycle 25. *Sol. Phys.* 295 (6), 1–17.
- Kopecký, M., 1950. Cycle de 22 ans de l'activité solaire. *Bull. Astron. Inst. Czech.* 2, 14.
- Labonville, F., Charbonneau, P., Lemerle, A., 2019. A dynamo-based forecast of solar cycle 25. *Sol. Phys.* 294 (6), 82.
- Lakhina, G.S., Tsurutani, B.T., 2018. Supergeomagnetic storms: past, present, and future. In: *Extreme Events in Geospace*. Elsevier, pp. 157–185.
- Macario-Rojas, A., Smith, K.L., Roberts, P.C., 2018. Solar activity simulation and forecast with a flux-transport dynamo. *Mon. Not. Roy. Astron. Soc.* 479 (3), 3791–3803.
- Muñoz-Jaramillo, A., Dasi-Espuig, M., Balmaceda, L.A., DeLuca, E.E., 2013. Solar cycle propagation, memory, and prediction: insights from a century of magnetic proxies. *Astrophys. J. Lett.* 767 (2), L25.
- Ohl, A., 1966. Forecast of sunspot maximum number of cycle 20. *Solice Danie* 9, 84.
- Pesnell, W.D., Schatten, K.H., 2018. An early prediction of the amplitude of solar cycle 25. *Sol. Phys.* 293 (7), 112.
- Pipin, V., Sokoloff, D., Usoskin, I., 2012. Variations of the solar cycle profile in a solar dynamo with fluctuating dynamo governing parameters. *Astron. Astrophys.* 542, A26.
- Riley, P., Baker, D., Liu, Y.D., Verronen, P., Singer, H., Güdel, M., 2018. Extreme space weather events: from cradle to grave. *Space Sci. Rev.* 214 (1), 21.
- Sarp, V., Kilcik, A., Yurchyshyn, V., Rozelot, J., Ozguc, A., 2018. Prediction of solar cycle 25: a non-linear approach. *Mon. Not. Roy. Astron. Soc.* 481 (3), 2981–2985.
- Singh, Y., et al., 2017. Short-and mid-term oscillations of solar, geomagnetic activity and cosmic-ray intensity during the last two solar magnetic cycles. *Planet. Space Sci.* 138, 1–6.
- Stefani, F., Stepanov, R., Weier, T., 2021. Shaken and stirred: when bond meets suess-de vries and gnevyshev-ohl. *Sol. Phys.* 296 (6), 1–23.
- Svalgaard, L., Cliver, E.W., Kamide, Y., 2005. Sunspot cycle 24: smallest cycle in 100 years? *Geophys. Res. Lett.* 32 (1).
- Thompson, R., 1993. A technique for predicting the amplitude of the solar cycle. *Sol. Phys.* 148 (2), 383–388.
- Tlatov, A.G., 2013. Reversals of gnevyshev-ohl rule. *Astrophys. J. Lett.* 772 (2), L30.
- Tsurutani, B.T., Gonzalez, W., Lakhina, G., Alex, S., 2003. The extreme magnetic storm of 1–2 september 1859. *J. Geophys. Res.: Space Phys.* 108 (A7).
- Upton, L.A., Hathaway, D.H., 2018. An updated solar cycle 25 prediction with aft: the modern minimum. *Geophys. Res. Lett.* 45 (16), 8091–8095.
- Zhuang, B., Wang, Y., Shen, C., Liu, R., 2018. A statistical study of the likelihood of a super geomagnetic storm occurring in a mild solar cycle. *Earth Planet. Phys.* 2 (2), 112–119.